

Briefing Space Weather

2022/06/20

1 Sun

1.1 Responsible: José Cecatto

06/13 – 1 M-3.5 flare; Fast wind stream (≤ 550 km/s); 7 CME c.h.c. toward the Earth;
06/14 – No flare (M/X); Fast wind stream (≤ 550 km/s); 8 CME c.h.c. toward the Earth;
06/15 – No flare (M/X); Fast wind stream (≤ 600 km/s); 3 CME c.h.c. toward the Earth;
06/16 – 1 M1.6 flare; Fast wind stream (≤ 600 km/s); 2 CME c.h.c. toward the Earth;
06/17 – No flare (M/X); Fast wind stream (≤ 700 km/s); 2 CME c.h.c. toward the Earth;
06/18 – No flare (M/X); Fast wind stream (≤ 600 km/s); No CME toward the Earth;
06/19 – No flare (M/X); Fast wind stream (≤ 650 km/s); 3 CME c.h.c. toward the Earth;
06/20 – No flare (M/X); Fast wind stream (≤ 650 km/s); No CME toward the Earth;
Prev.: Fast wind stream up to June 21; for the next 2 days low (25% M, 05% X) probability of M / X flares; also, occasionally other CME can present component toward the Earth.
c.h.c. – can have a component; * partial halo; ** halo

2 Sun

2.1 Responsible: Douglas Silva

- WSA-ENLIL (Prediction for CMEs 2022-06-10T00:06Z, 2022-06-09T21:24Z)
 - The simulation results indicate that the flanks of combined Coronal Mass Ejections will reach the DSCOVR mission between 2022-06-12T13:17Z and 2022-06-13T03:17Z.
- WSA-ENLIL (CME 2022-06-13T03:12Z)
 - The simulation results indicate that the flank of CME will reach the DSCOVR mission between 2022-06-14T17:21Z and 2022-06-15T07:21Z.

Buracos coronais (SPoCA : Spatial Possibilistic Clustering Algorithm):

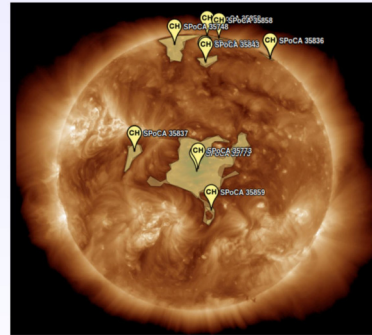
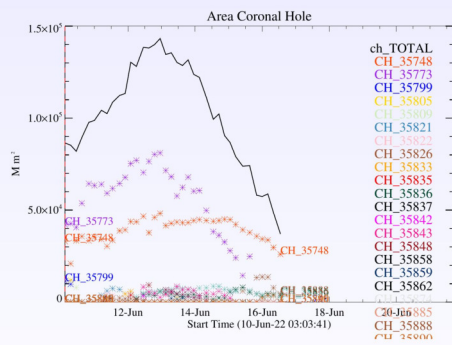
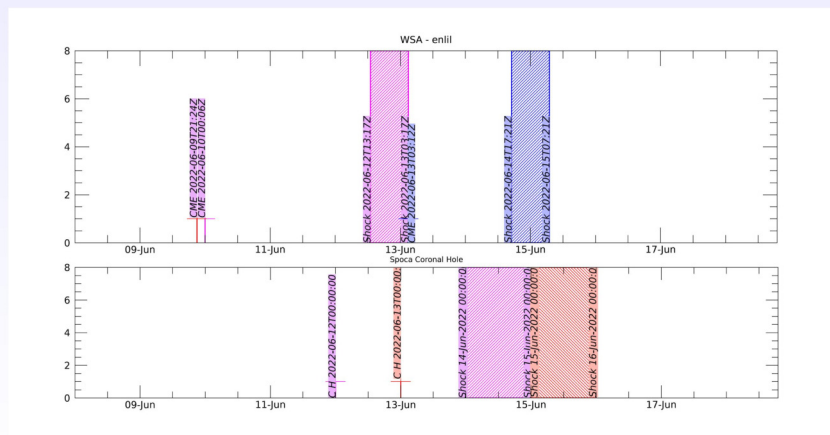


Figura: A linha em preto mostra o resultado da soma das areas para cada intervalo da detecção realizado pelo SPOCA entre os dias 10 de junho e 18 de junho de 2022

Sobre a imagem em 193 Å do Sol estão destacados os Buracos coronais observados pelo SPOCA por volta das 00:00 UT do dia 12 de junho de 2022.



WSA - ENLIL SPOCA

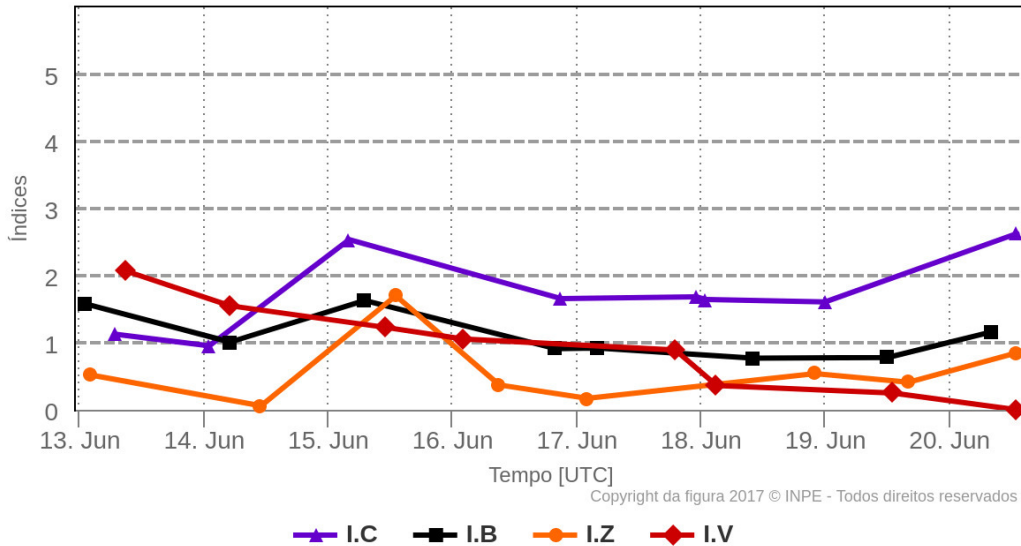


3 Interplanetary Medium

3.1 Responsible: Paulo Jauer

Resumo dos índices do meio interplanetário

Máximos diários - mais recentes entre 13 Jun, 2022 e 20 Jun, 2022



- The interplanetary medium region in the last week showed a low/moderate level of plasma perturbations due to the possible interaction of CME and HSS-like structures identified by the DISCOVERY satellite in the interplanetary medium.
- The modulus of the interplanetary magnetic field component showed 1 maximum peak on June 15th at 03:30 from ~ 12.45 nT.
- The BxBy components showed variations in the analyzed period, both remaining oscillating within the $[+11, -11]$ nT interval, without the presence of sector switching.
- The component of the bz field showed fluctuations oscillating mostly in the $[+5,-5]$ nT interval. The bz component showed an abrupt variation of ~ -6.72 nT on June 15th at 1:30 pm due to an ICME interaction.
- The solar wind density peaked on June 15 at 04:30 at $21.52 p/cm^3$. The density remained oscillating below $11 p/cm^3$ in the rest of the period.
- The solar wind speed fluctuated above 400 km/s throughout the period, with a maximum peak of 602 km/s on June 15 at 02:30.
- The position of the magnetopause was oscillating on average and below the equilibrium position. On June 15 at 04:30, it presented a maximum compression of 7.75 Re.

4 Radiation Belts

4.1 Responsible: Ligia Alves da Silva

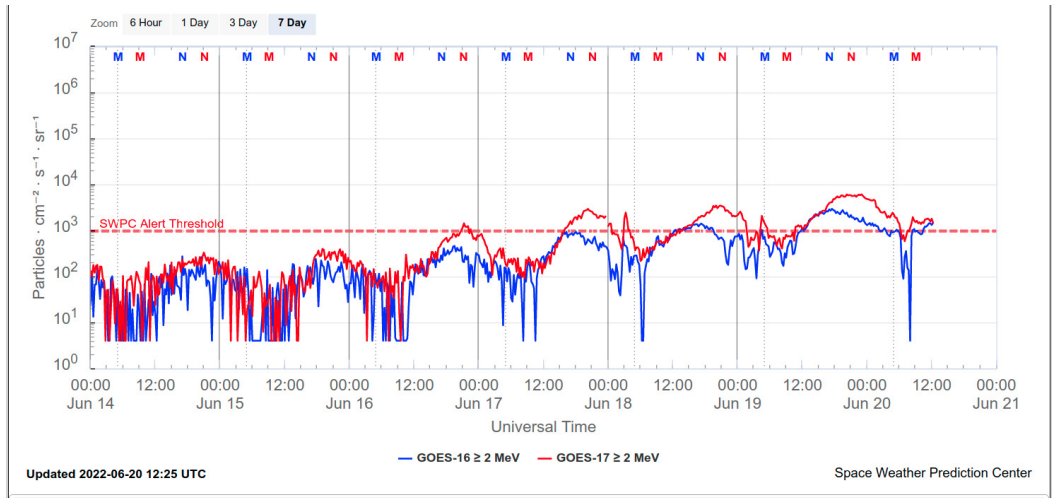


Figura 1: High-energy electron flux ($\geq 2\text{MeV}$) obtained from GOES-16 and GOES-17 satellite. Source: <https://www.swpc.noaa.gov/products/goes-electron-flux>.

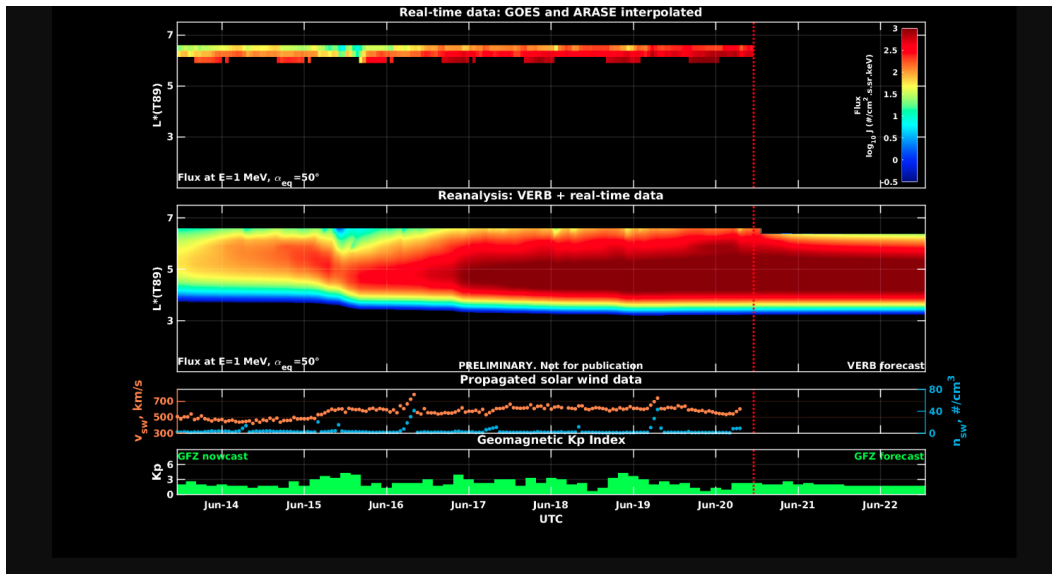


Figura 2: high-energy electron flux data (real-time and interpolated) obtained from ARASE, GOES-16, GOES-17 satellites. Reanalysis's data from VERB code and interpolated electron flux. Solar wind velocity and proton density data from ACE satellite. Source: <https://rbm.epss.ucla.edu/realtime-forecast/>.

High-energy electron flux ($\geq 2\text{ MeV}$) in the outer boundary of the outer radiation belt obtained from geostationary satellite data GOES-16 and GOES-17 (Figure 1) is close to 10^2 particles/(cm^2sr) up to 12:00 UT on June 16th, increasing gradually its population until reaching values close to 10^4 particles/(cm^2sr) on June 19th.

The GOES-16, GOES-17, and Arase satellite data are analyzed and interpolated to observe the high-energy electron flux variability (1 MeV) in the outer radiation belt (Figure 2). Additionally, the VERB code rebuilds this electron considering the Ultra Low Frequency (ULF) waves' radial diffusion. The simulation (VERB code) shows that the electron flux decreases on June 15th from L-shell = 6.0, followed by an increase that was more significant in the inner L-shells. The electron flux variabilities occurred concomitantly with the ULF wave activities.

5 ULF waves

5.1 Responsible: Graziela B. D. Silva

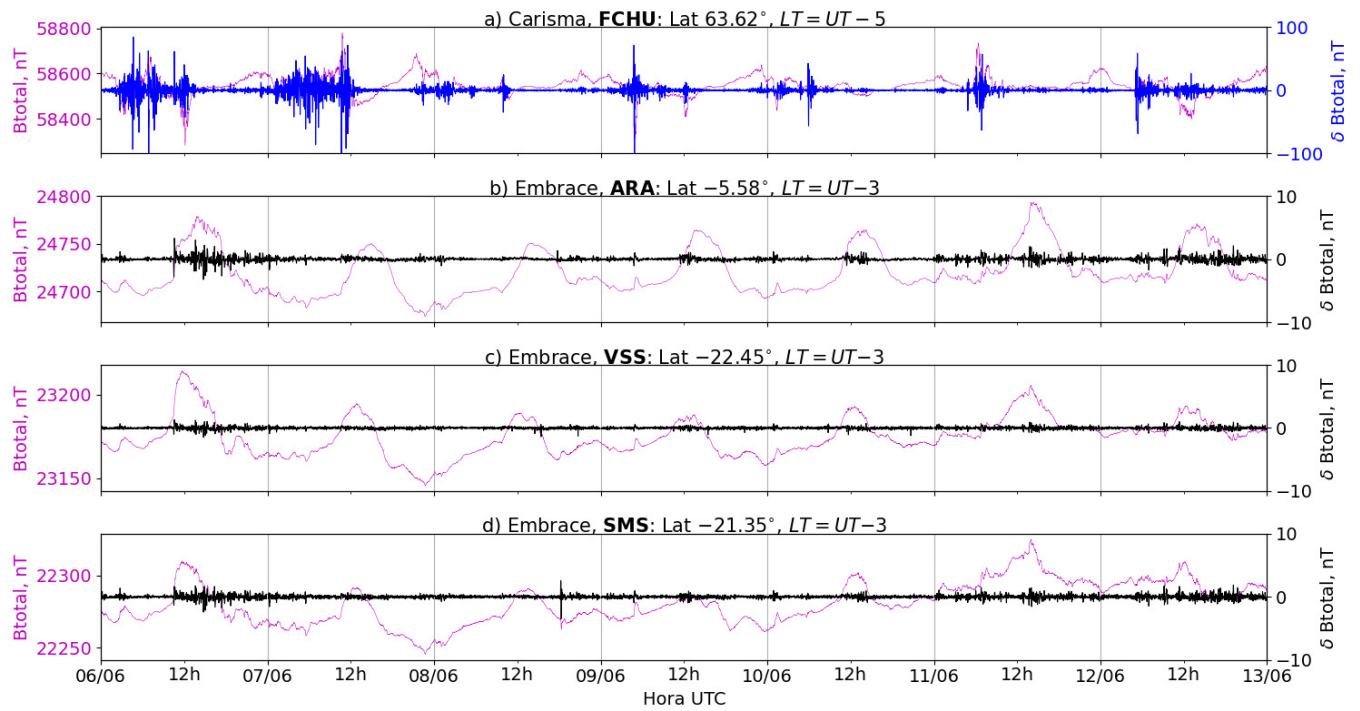


Figura 3: a) Timeseries of the geomagnetic field total component measured at FCHU station (Fort Churchill) of the CARISMA magnetometer network in magenta, along with the associated perturbation in the Pc5 band shown in blue. b-d) timeseries of the geomagnetic field total component measured at stations ARA (Araguatins), VSS (Vassouras) and SMS (São Martinho da Serra) of the EMBRACE network in magenta, along with the Pc5 perturbation in blue.

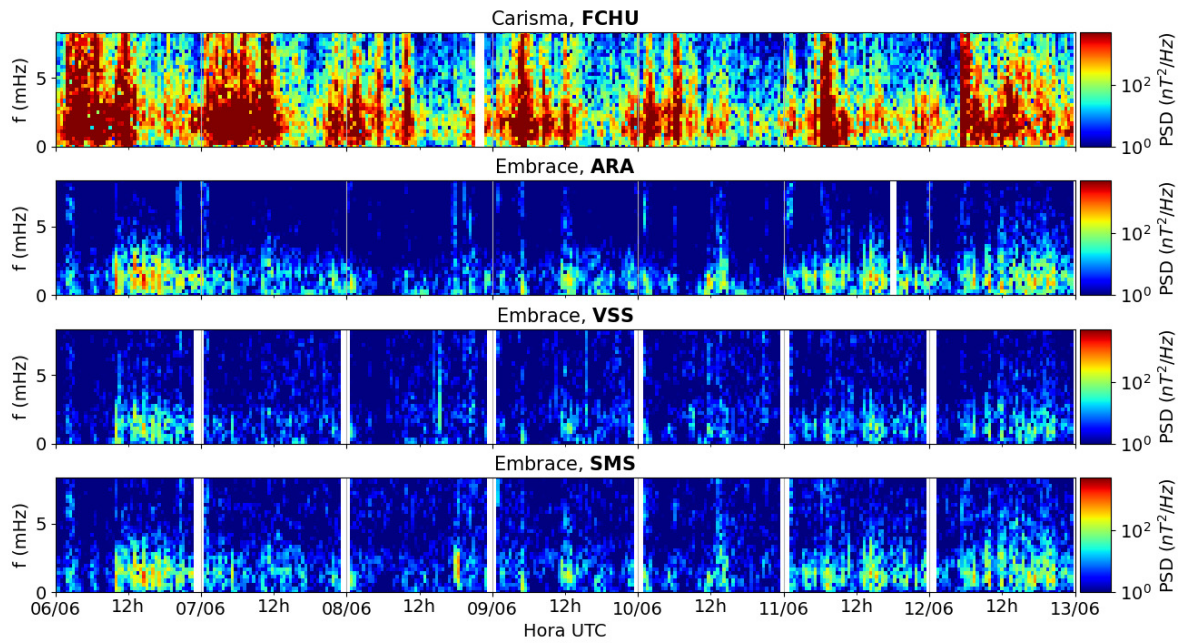


Figura 4: a-d) Time evolution of the power spectral density obtained from the filtered timeseries of the geomagnetic field total component (δB_{total}) for a) the high latitude station (FCHU-CARISMA), and b-d) for the low latitude stations of EMBRACE (ARA, VSS, SMS).

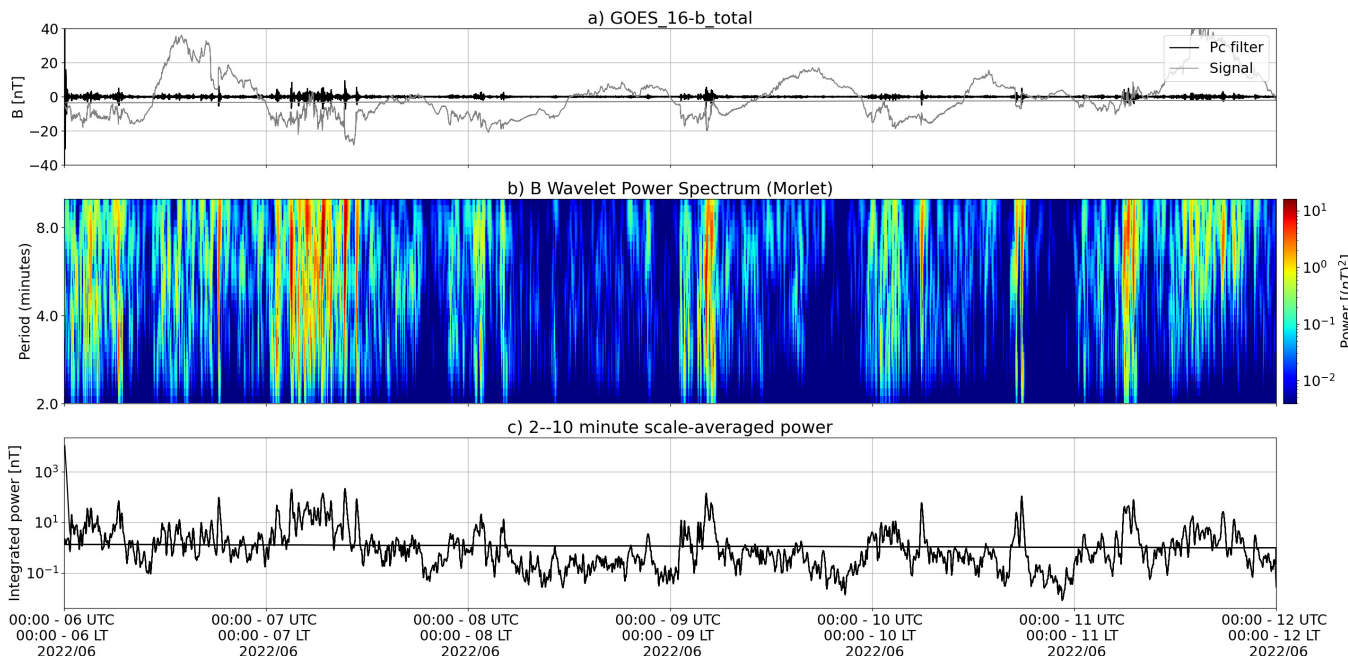


Figura 5: a) Timeseries of the geomagnetic field total component measured by GOES 16, together with the Pc5 fluctuation in black. b) Wavelet power spectrum of the filtered timeseries. c) Average ULF power in the period range from 2 to 10 minutes.

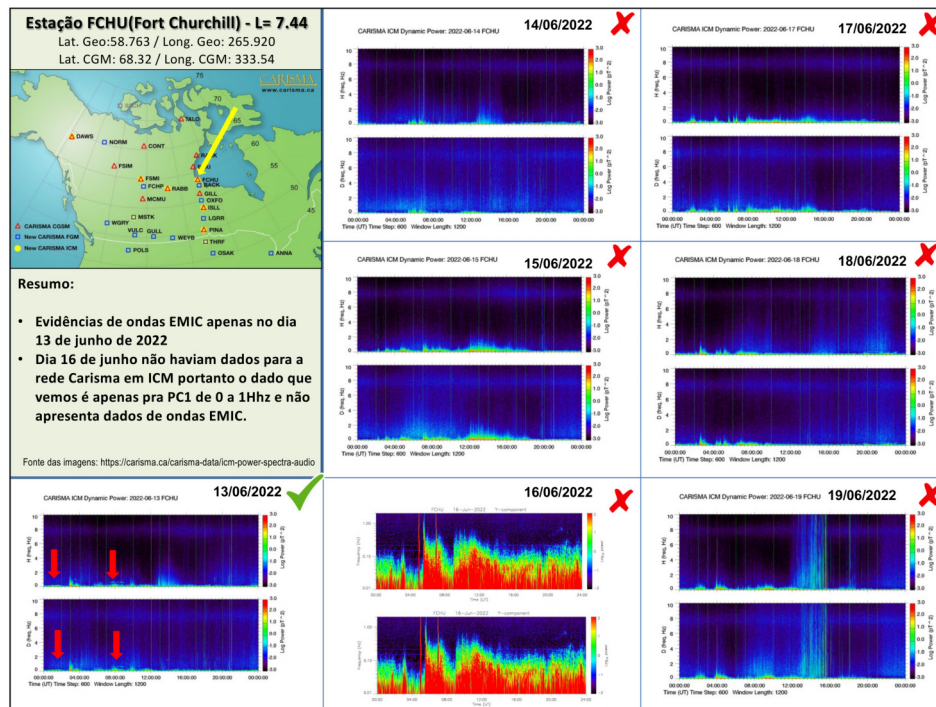
- There was a rapid ULF wave pulse on 13/june followed by intense and continuous activity of Pc5 ULF waves between 15/june and 18/june, as measured by GOES 16 at geosynchronous orbit ($L \sim 6.6$). The wave activity was associated with the arrival of interplanetary shocks on 13/june and

15/june, together with ICME (interplanetary coronal mass ejection) on 15/june.

- For the ground-based stations, the same wave pulse on 13/june followed by an intense activity of ULF waves were registered through 15-19/june both in Fort Churchill (FCHU/high latitude) and at the EMBRACE low-latitude stations.
- Specifically on 15/june, another rapid pulse was registered down to low latitudes, reaching amplitudes up to $[+10,-10]$ nT, especially at ARA and SMS stations.

6 Ondas EMIC

6.1 Responsible: Claudia Medeiros



7 Geomagnetic activity

7.1 Responsible: Lívia Alves

In the week of 14-20 June, the following events related to geomagnetic activity stand out:

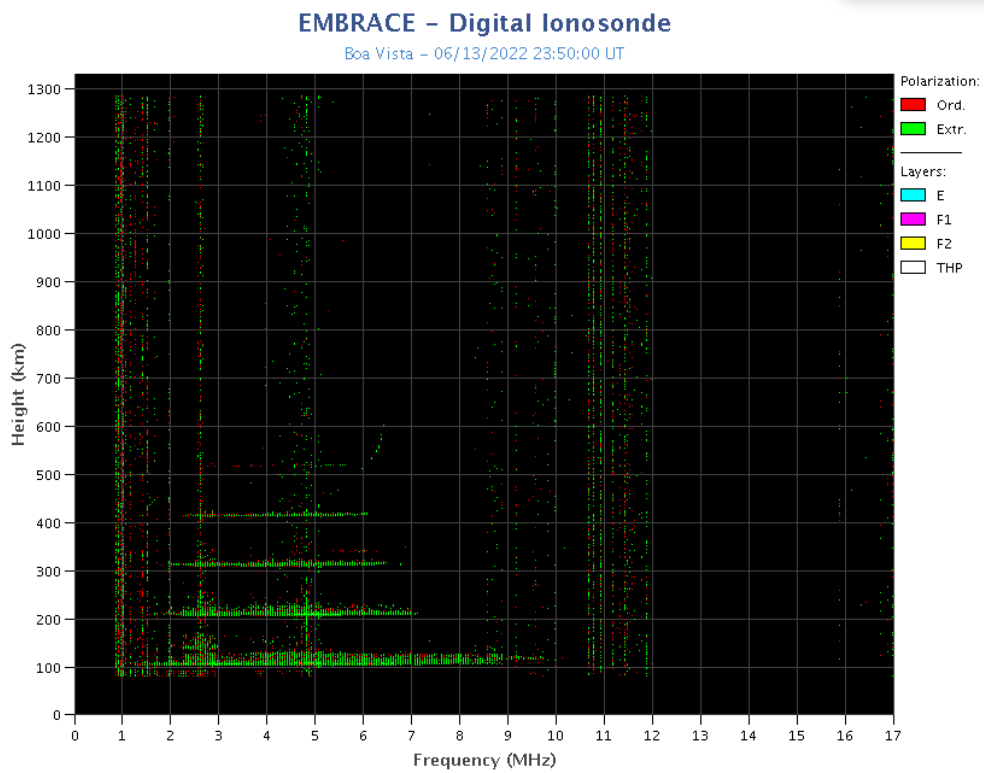
- The data from the Embrace magnetometer network showed instabilities throughout the period, with emphasis on Jun 15 - The magnetometers of the Embrace network recorded a drop followed by an enhancement in the H component.
- The geomagnetic activity was unstable throughout the period, the AE index was unsettled in the period, AE index reached 1000 nT. The Dst index reached -30 nT. The highest Kp of the week was 4+.
- The geomagnetic field measured at the GOES orbit shows instabilities on 15 and 16-June.

8 Ionosphere

8.1 Responsible: Laysa Resende

Boa Vista:

- There were not occurred spread F during this week.
- The Es layers reached scale 5 on June 13.

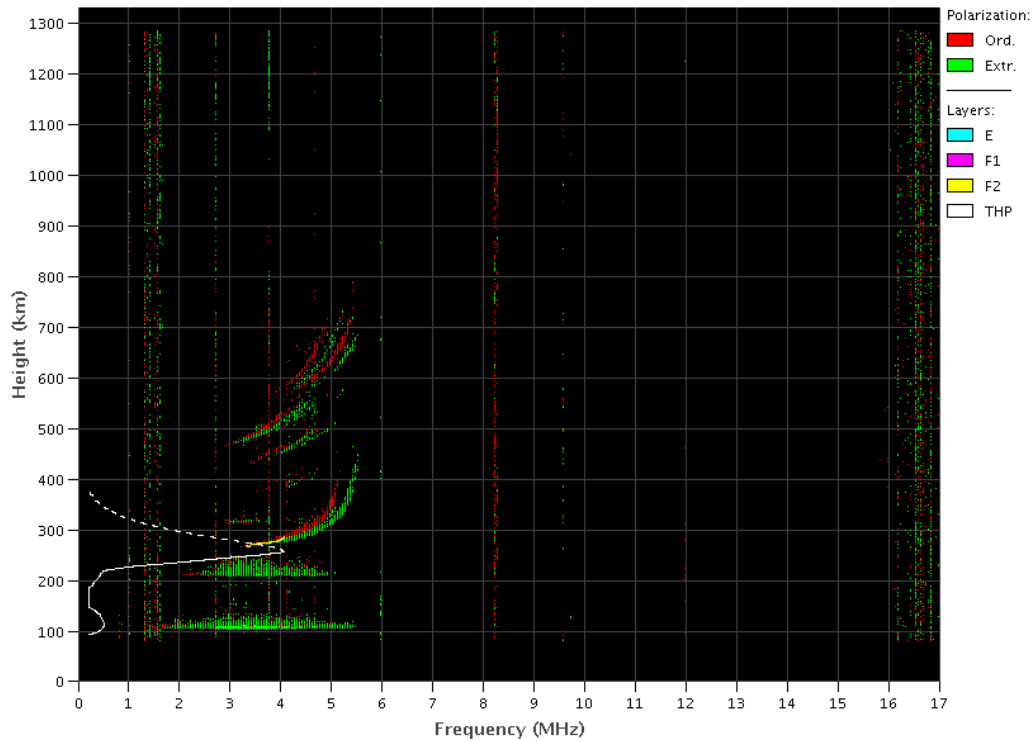


Cachoeira Paulista:

- There were not occurred spread F during this week.
- The Es layers reached scale 3 on June 14, 18, and 19.

EMBRACE – Digital Ionosonde

Cachoeira Paulista – 06/19/2022 23:50:00 UT

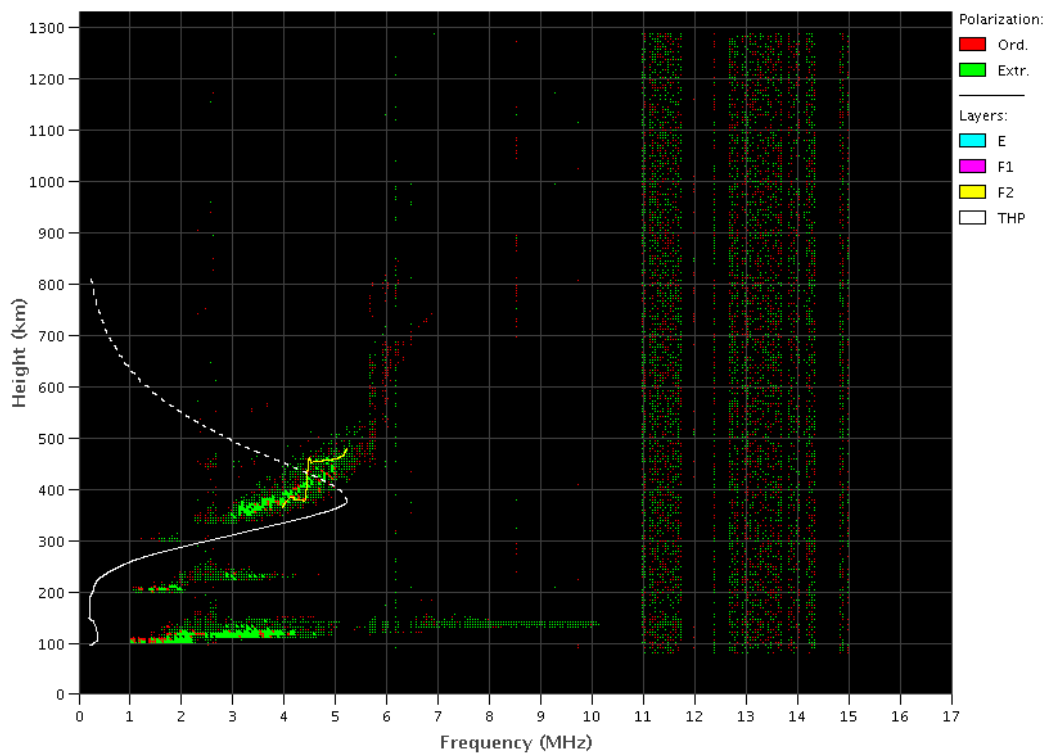


São Luís:

- There were a weak spread F during this week.
- The Es layers reached scale 4 on day 17, and 19.

EMBRACE – Digital Ionosonde

São Luís – 05/11/2022 01:40:00 UT



9 All-Sky Imager

9.1 Responsible: LUME

All-Sky Imager EPBs Observation
Observações das EPBs por meio do imageador All-Sky
June 13- June 19, 2022 || 13 de junho- 19 de junho, 2022

Observatory	June 13	June 14	June 15	June 16	June 17	June 18	June 19
Observatório	junho 13	junho 14	junho 15	junho 16	junho 17	junho 18	junho 19
CA	✗	✓☁○	✓☁☽	✓☁☽	✓☁☽	✓☁☽	✓☁☽
BJL	✗	✗	✗	✗	✗	✗	✗
CP	✓☁☽	✓☁○	✓☁☽	✓☁☽	✓☁☽	✓☁☽	✓☁☽
SMS	✗	✗	✗	✗	✓☁☽	✓☁☽	✓☁☽
Definition of Symbols							
CA	São João do Cariri						
BJL	Bom Jesus da Lapa						
CP	Cachoeira Paulista						
SMS	São Martinho da Serra						
✓	Observation - Observação						
✗	No Observation - Sem Observação						
○	Clear sky - Céu limpo						
☁	Partly Cloudy - Parcialmente Nublado						
☽	Cloudy - Nublado						

- At the Sao Joao do Cariri observatory no geophysical phenomena such as plasma bubbles and traveling ionospheric disturbances were observed during the period. On day 13, there were no observations.
- At the Bom de Jesus da Lapa observatory there was no observation due to technical problems.
- At the Cachoeira Paulista observatory no geophysical phenomena such as plasma bubbles and traveling ionospheric disturbances were observed during the period. The sky was cloudy throughout the week.
- Finally, at the observatory of Sao Martinho da Serra observatory, no geophysical phenomena such as plasma bubbles and traveling ionospheric disturbances were observed during the period. On days 13, 14, 15 and 16, there were no observations.

TEC

- No plasma bubbles were observed during the entire period. Besides, the equatorial anomaly was observed every day.